

Zhao Liu, Zhongzhou Chen and
Wei Wu*State Key Laboratory of Agrobiotechnology,
College of Biological Sciences, China
Agricultural University, Beijing 100193,
People's Republic of China

Correspondence e-mail: wuweiyu@cau.edu.cn

Received 17 April 2012
Accepted 28 May 2012

Crystallization and preliminary X-ray studies of ferric uptake regulator from *Magnetospirillum gryphiswaldense*

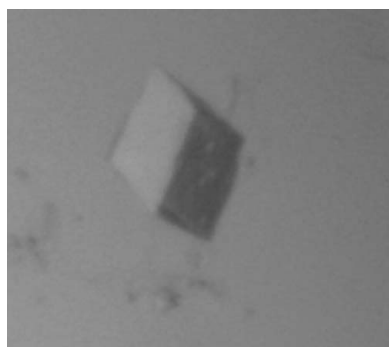
Magnetosomes in magnetotactic bacteria have been widely used in studies of magnetic domains and in commercial applications. The iron content of magnetotactic bacteria is ~ 100 times higher than that of *Escherichia coli*. *Magnetospirillum gryphiswaldense* MSR-1 can still take up iron even at high intracellular concentrations. Ferric uptake regulator (Fur) is a global iron-responsive regulator that affects magnetosome formation, iron transport and oxygen metabolism. However, the mechanism of iron uptake and homeostasis by *M. gryphiswaldense* MSR-1 Fur is not clear. Here, the expression, purification and crystallization of apo and SeMet Fur from *M. gryphiswaldense* MSR-1 are reported. The crystals belonged to space group *C2*. Matthews coefficient analysis and size-exclusion chromatography showed that the asymmetric unit probably contains one dimer of Fur. Diffraction data were optimized to 1.58 Å resolution for apo Fur and to 1.9 Å resolution for SeMet Fur.

1. Introduction

Magnetotactic bacteria are a heterogeneous group of aquatic prokaryotes with a unique intracellular organelle, the magnetosome, which consists of chains of magnetite (Fe_3O_4) crystals and orients the cell along magnetic field lines (Blakemore, 1975; Scheffel *et al.*, 2006). The magnetite crystals are nanometre-sized, uniform, well dispersed, membrane-bound and nontoxic. These features endue magnetosomes with an inestimable potential commercial value for application in many fields including new materials research and medicine development. The formation of magnetosomes involves the uptake and intracellular accumulation of large amounts of iron. Magnetotactic bacteria consist of up to 3% iron as measured by dry weight. Excessive uptake of iron, on the other hand, may lead to oxidative damage from the generation of dangerous radicals by oxygen and iron. Therefore, a unique mechanism for assimilation and utilization of iron from the environment is needed in magnetotactic bacteria.

The most common and best characterized transcriptional regulator of genes involved in iron uptake, storage and metabolism in bacteria is ferric uptake regulator (Fur). In *Escherichia coli*, more than 90 genes have been found to be regulated by Fur (Hantke, 2001). Fur is a global regulator that acts as a transcriptional repressor when it binds ferrous ion. When the concentration of free ferrous ion is high, Fur forms a complex with Fe^{2+} . The metal-bound Fur binds to an ~ 20 bp DNA sequence ('Fur box') and suppresses the transcription of target genes involved in the iron-uptake system, resulting in cessation of iron uptake. When the free Fe^{2+} concentration is low, metal-bound Fur dissociates from Fe^{2+} and leaves the promoters, thus inducing transcription.

M. gryphiswaldense MSR-1 can be cultivated more readily than most other magnetotactic bacteria (Schultheiss & Schüler, 2003) and studies have therefore increasingly focused on it. It has recently been demonstrated that *M. gryphiswaldense* MSR-1 Fur (MSR-1 Fur) is a global iron-responsive regulator that affects magnetosome formation and directly regulates the expression of several key genes involved in iron transport and oxygen metabolism (Qi *et al.*, 2012; Uebe *et al.*,



2011). MSR-1 Fur has been shown to directly regulate the transcription of catalase-peroxidase and superoxide dismutase for oxygen metabolism and the *feoAB1* and *feoAB2* genes for the uptake of metal ions. Sequence alignment showed that MSR-1 Fur shares low sequence identity with other known Furs. Magnetotactic bacteria have a high iron content of ~100 times that of *E. coli*. Little is known regarding the mechanisms by which they efficiently acquire sufficient iron for magnetosome production and avoid the generation of toxic radicals from excess free iron at their unusually high intracellular iron contents (Bazylnski & Frankel, 2004; Frankel *et al.*, 1979). Moreover, the unusually high iron content of *M. gryphiswaldense* MSR-1 makes it a useful model for the study of the biological mechanisms of iron uptake and homeostasis. Therefore, it is not clear whether the mechanism of *E. coli* Fur is applicable to MSR-1 Fur. These questions triggered our interest in elucidating the mechanism of MSR-1 Fur in response to high concentrations of iron. Here, crystals of apo and SeMet MSR-1 Fur were successfully obtained and X-ray data were collected to 1.58 and 1.9 Å resolution, respectively.

2. Materials and methods

2.1. Protein expression

The Fur gene was amplified from the *M. gryphiswaldense* cDNA library. The amplified fragment corresponding to MSR-1 Fur was inserted into the *NdeI*–*XhoI* sites of the pET-28a vector (EMD), in which the thrombin recognition site was replaced by a tobacco etch virus (TEV) protease recognition site. The recombinant DNA plasmids were transformed into *E. coli* strain JM109 competent cells, which were selected using kanamycin. Target gene sequences of positive colonies were verified by DNA sequencing. The correct plasmids were transformed into *E. coli* strain BL21 (DE3) (EMD) for protein expression.

Freshly transformed *E. coli* cells were incubated in 5 ml Luria–Bertani (LB) medium at 310 K overnight. The incubated cells were then transferred to 1 l LB medium at 310 K supplemented with 25 mg ml⁻¹ kanamycin. When the optical density at 600 nm (OD₆₀₀) reached 0.8, 0.1 mM isopropyl β-D-1-thiogalactopyranoside (IPTG) was added to induce expression for an additional 12 h at 289 K. Selenomethionyl (SeMet) MSR-1 Fur was prepared similarly in non-autoinducing selenomethionine minimal medium (Studier, 2005) with 100 mg l⁻¹ seleno-L-methionine (Sigma). The medium consisted of 1 g NH₄Cl, 3 g KH₂PO₄ and 6 g Na₂HPO₄ supplemented with 20% (w/v) glucose, 0.3% (w/v) MgSO₄ and 10 mg FeSO₄ in 1 l double-distilled water. Induction was carried out at 293 K for 24 h by the addition of 0.1 mM IPTG.

2.2. Protein purification

The cells were harvested by centrifugation at 4000 rev min⁻¹ for 15 min, resuspended in lysis buffer (20 mM Tris–HCl pH 8.0, 500 mM NaCl) and lysed by sonication. The lysate was centrifuged at 20 000 rev min⁻¹ for 20 min and the supernatant was filtered through a 0.45 μm filter membrane to remove cell debris and other impurities. The protein was purified by immobilized metal-affinity chromatography (IMAC) on a nickel column (Sigma) and was eluted with a 50–300 mM imidazole gradient in lysis buffer. The His tag and linker region were cleaved from MSR-1 Fur using TEV protease at 277 K for 16 h and were removed by IMAC. For crystallization, the MSR-1 Fur protein was further purified by size-exclusion chromatography (Superdex 200, GE Healthcare) equilibrated with lysis buffer. Purification of the SeMet MSR-1 Fur protein was performed using the same protocols.

Table 1

Data-collection and processing statistics.

Values in parentheses are for the highest resolution shell.

| | SeMet MSR-1 Fur, MAD data set | | | |
|----------------------------------|--|------------------------|------------------------|--|
| | Peak | Inflection | Remote | Apo MSR-1 Fur |
| X-ray source | BL17U, SSRF | | | NE3A, Photon Factory |
| Space group | C2 | | | C2 |
| Unit-cell parameters (Å, °) | $a = 69.2, b = 78.7, c = 66.1,$ $\alpha = \gamma = 90, \beta = 108.9$ | | | $a = 69.2, b = 78.1,$ $c = 65.9,$ $\alpha = \gamma = 90,$ $\beta = 108.7$ |
| Wavelength (Å) | 0.9793 | 0.9795 | 1.000 | 1.000 |
| Resolution (Å) | 50–1.90 (1.93–1.90) | 50–1.85 (1.88–1.85) | 50–1.60 (1.63–1.60) | 50–1.58 (1.61–1.58) |
| $R_{\text{merge}}^{\dagger}$ (%) | 6.0 (37.7) | 5.4 (23.8) | 6.6 (49.4) | 6.7 (48.5) |
| $\langle I/\sigma(I) \rangle$ | 46.2 (3.2) | 52.5 (6.1) | 53.0 (2.3) | 52.5 (2.1) |
| Completeness (%) | 98.7 (88.7) | 98.1 (80.0) | 99.1 (92.1) | 98.5 (84.4) |
| Multiplicity | 7.4 (4.6) | 7.3 (5.7) | 7.9 (4.4) | 7.9 (4.0) |

$\dagger R_{\text{merge}} = \frac{\sum_{hkl} \sum_i |I_i(hkl) - \langle I(hkl) \rangle|}{\sum_{hkl} \sum_i I_i(hkl)}$, where $I_i(hkl)$ is the i th observed intensity of reflection hkl and $\langle I_i(hkl) \rangle$ is the average intensity over symmetry-equivalent measurements.

2.3. Crystallization

For crystallization, the protein was concentrated to 10 mg ml⁻¹ in 20 mM Tris–HCl pH 8.0, 50 mM NaCl, 1 mM tris(2-carboxyethyl)-phosphine (TCEP) using an Amicon Ultra-10 device (Millipore). Initial crystallization trials were performed using sitting-drop vapour diffusion in 48-well plates (Hampton Research) at 293 K. The crystallization conditions used were from commercial crystallization kits (Hampton Research and Emerald BioStructures). The crystallization drop was composed of 1 μl well solution and 1 μl freshly purified protein solution and was equilibrated against 400 μl well solution. The small needle-shaped crystals obtained from the initial crystallization trials were further refined by the hanging-drop vapour-diffusion method. After extensive optimization, diffracting crystals were obtained using a reservoir consisting of 1.8 M ammonium sulfate, 0.1 M sodium citrate pH 5.5. SeMet MSR-1 Fur was crystallized using 1.4 M ammonium sulfate, 0.1 M sodium citrate pH 5.5. SeMet and apo MSR-1 Fur crystals were cryoprotected by a brief transfer into their respective reservoir solutions supplemented with glycerol to a final concentration of 20% and were then flash-cooled in liquid nitrogen.

2.4. Data collection and processing

MSR-1 Fur diffraction data were collected to 1.58 Å resolution on beamline NE3A at Photon Factory (KEK) at 1.000 Å wavelength. X-ray absorption spectra were recorded on beamline BL17U at the Shanghai Synchrotron Radiation Facility (SSRF) equipped with an Si(111) double-crystal monochromator and a fluorescence detector containing 15 elements. The spectra were recorded around the Mn, Fe, Co, Ni, Cu, Zn and Se K edges from 6000 to 13 000 eV. Data analysis was performed using the software *CHOOCH* (Evans & Pettifer, 2001). A three-wavelength MAD data set was collected from SeMet MSR-1 Fur crystals at the Se K edge (0.9793, 0.9795 and 1.0000 Å) on beamline BL17U. The synchrotron-radiation experiments were performed at 100 K and the CCD detector was fixed at a distance of 200 mm. Data collection from the crystals was performed using an angular range of 360° with an oscillation step of 1.0° and an exposure time of 0.5 s. All data were integrated and scaled with the *HKL-2000* suite of programs (Otwinowski & Minor, 1997). The final MAD data sets in space group C2 were processed to a cutoff of 1.90 Å based on significant drops in the unaveraged $I/\sigma(I)$ (<2.0) and

completeness (<80%) in the higher resolution shells. Data-collection statistics are summarized in Table 1.

3. Results and discussion

His-tagged MSR-1 Fur protein was successfully subcloned, expressed and purified by affinity chromatography. The His tag was removed from the recombinant protein by TEV protease and was separated from the protein by gel-exclusion chromatography. SDS-PAGE analysis showed that the proteins were highly purified and homogenous. Apo MSR-1 Fur protein was concentrated to 10 mg ml⁻¹ for crystallization. Initial crystallization trials were performed using a large number of crystallization conditions. Condition No. 32 (2.0 M ammonium sulfate) of Crystal Screen from Hampton Research gave many small needle-shaped crystals. The crystallization conditions, including the buffer type, pH, precipitant concentrations, additives

and temperature, were extensively optimized. Rod-shaped crystals (Fig. 1a) were obtained using a reservoir consisting of 2.0 M ammonium sulfate, 0.1 M sodium citrate pH 5.0 after 2 d of growth. However, these crystals were small and were unsuitable for diffraction studies; for example, the resolution of the rod-shaped crystals was about 10 Å. To improve the crystal quality, the seeding technique (Rangarajan & Izard, 2010) was used. A seed stock was made by crushing two rod-shaped crystals in the mother liquor and was diluted 1000–10 000 times. Many crystal nuclei appeared after 2 d at 293 K in a 2 µl droplet made by mixing equal volumes of protein solution and well solution. To reduce the formation of so many crystal nuclei, the crystallization conditions were further optimized. Moreover, fresh protein and well solution supplemented with various concentrations of glycerol were ultracentrifuged at 20 000 rev min⁻¹ for 1 h, which was immediately followed by the set-up of crystal experiments. After extensive efforts involving four rounds of seeding and the addition of various concentrations of glycerol, the optimal condition was found

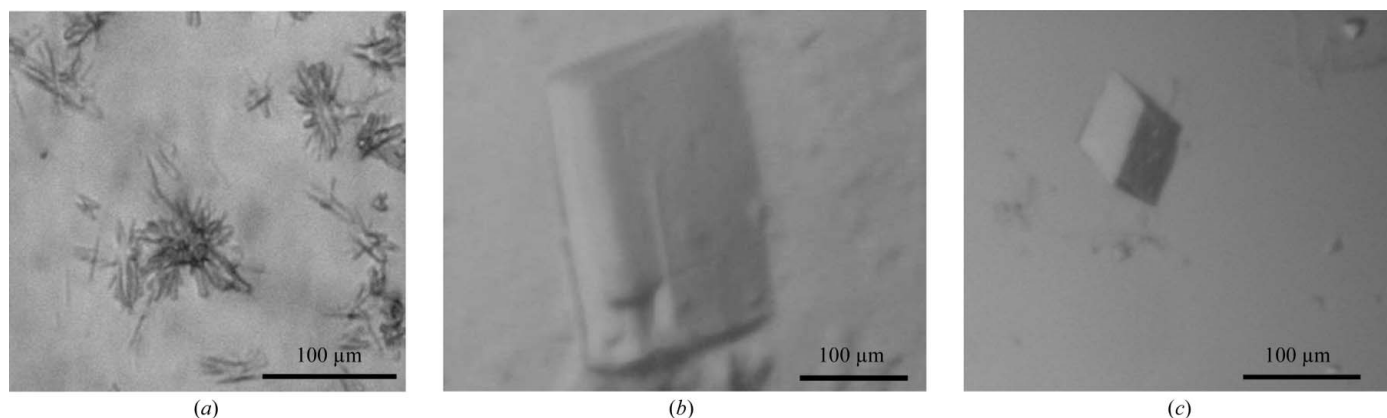


Figure 1 Crystallization of MSR-1 Fur. (a) Apo MSR-1 Fur crystals after optimization of crystallization conditions, (b) crystals of apo MSR-1 Fur after seeding and (c) crystals of SeMet MSR-1 Fur after seeding.

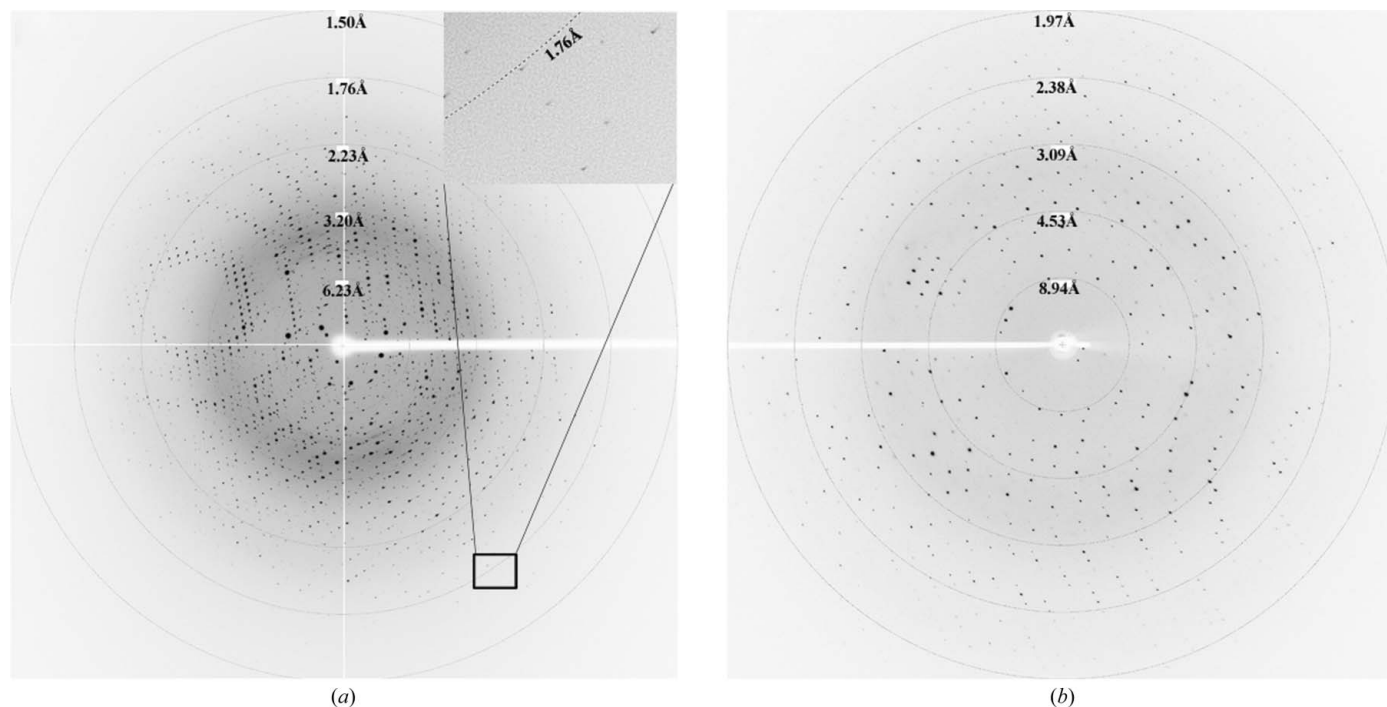


Figure 2 X-ray diffraction images from (a) apo MSR-1 Fur and (b) SeMet MSR-1 Fur crystals.

to be 1.8 M ammonium sulfate and 0.1 M sodium citrate pH 5.5 with 10% glycerol. After 3 d of growth without any interference, the best crystal was a large triangular prism (Fig. 1*b*). It diffracted to 1.58 Å resolution in space group *C2* (Fig. 2*a*). Matthews coefficient analysis showed that two MSR-1 Fur protomers in the asymmetric unit would be reasonable (Table 1), consistent with the observation that MSR-1 Fur is a dimer in solution from size-exclusion chromatography.

Next, we tried to calculate an initial electron-density map from the 1.58 Å resolution data set of MSR-1 Fur. A *BLAST* search (Altschul *et al.*, 1990) of current PDB structures yielded several high hits, such as *Pseudomonas aeruginosa* Fur (Pohl *et al.*, 2003; PDB entry 1mzb) and *Vibrio cholerae* Fur (Sheikh & Taylor, 2009; PDB entry 2w57). Initial attempts to solve the MSR-1 Fur structure by molecular replacement as implemented in *Phaser* (McCoy, 2007), *MOLREP* (Vagin & Teplyakov, 2010) and *AMoRe* (Trapani & Navaza, 2008) within the *CCP4* suite (Winn *et al.*, 2011) using dimers or monomers of hits from *BLAST* (such as PDB entries 1mzb or 2w57) as search models did not succeed. Alignment of the MSR-1 Fur sequence with those of *P. aeruginosa* Fur and *V. cholerae* Fur showed 32 and 28% sequence identity, respectively. Therefore, these sequences did not have significant homology to that of MSR-1 Fur. Most importantly, the X-ray absorption spectra of MSR-1 Fur indicated that there were no divalent metal ions in the crystal. Therefore, the structure of MSR-1 Fur is an apo structure. In contrast, all solved Fur structures contain two or four metal ions. Thus, the structure of apo MSR-1 Fur might differ from the solved metal-bound Fur structures. To attempt to solve the structure of MSR-1 Fur, heavy-atom soaking was carried out. Several conventional haloids and metal salts such as platinate and mercuric compounds were tested. However, none of them was successful.

Initial efforts to crystallize SeMet MSR-1 Fur using the optimized crystallization condition for apo MSR-1 Fur produced crystals that diffracted to only 8 Å resolution. After extensive seeding screening as used for apo MSR-1 Fur, SeMet MSR-1 Fur crystals were grown using a well buffer consisting of 1.4 M ammonium sulfate, 0.1 M sodium citrate pH 5.5. The crystals were large, with sharp and regular edges (Fig. 1*c*). There was no obvious difference in crystal appearance between apo and SeMet MSR-1 Fur crystals. The diffraction intensity of SeMet MSR-1 Fur also demonstrated that the crystal packing was highly ordered. The best crystal diffracted to 1.9 Å resolution and belonged to space group *C2* (Fig. 2*b*). The X-ray absorption spectra of SeMet MSR-1 Fur indicated the presence of selenium. In contrast, divalent metal ions such as Mn²⁺, Fe²⁺, Co²⁺, Ni²⁺, Cu²⁺ and Zn²⁺ were not detected, as in apo MSR-1 Fur. Data analysis using

CHOOCH (Evans & Pettifer, 2001) indicated that the peak and inflection wavelengths of the SeMet MSR-1 Fur crystal were 0.9793 and 0.9795 Å, respectively, and these wavelengths were used to collect a three-wavelength MAD data set.

Analysis of these data indicated a solvent content of 52.6% and a Matthews coefficient of 2.59 Å³ Da⁻¹, corresponding to two SeMet MSR-1 Fur molecules per asymmetric unit (Table 1). The positions of the six Se atoms in the asymmetric unit and a subsequent electron-density map were determined using *SHARP* (Vonnrhein *et al.*, 2007). Detailed structure determination and biochemical experiments on iron uptake and homeostasis in *M. gryphiswaldense* MSR-1 are currently in progress.

The project was supported by the National Basic Research Program of China (973 Program, 2011CB965304 and 2009CB825501), the National Natural Science Foundation of China (30870494 and 31070664) and the Scientific Research Starting Foundation for Returned Overseas Chinese Scholars. We thank Professor Ying Li of China Agricultural University for providing Fur cDNA.

References

- Altschul, S. F., Gish, W., Miller, W., Myers, E. W. & Lipman, D. J. (1990). *J. Mol. Biol.* **215**, 403–410.
- Bazylnski, D. A. & Frankel, R. B. (2004). *Nature Rev. Microbiol.* **2**, 217–230.
- Blakemore, R. (1975). *Science*, **190**, 377–379.
- Evans, G. & Pettifer, R. (2001). *J. Appl. Cryst.* **34**, 82–86.
- Frankel, R. B., Blakemore, R. P. & Wolfe, R. S. (1979). *Science*, **203**, 1355–1356.
- Hantke, K. (2001). *Curr. Opin. Microbiol.* **4**, 172–177.
- McCoy, A. J. (2007). *Acta Cryst.* **D63**, 32–41.
- Otwinowski, Z. & Minor, W. (1997). *Methods Enzymol.* **276**, 307–326.
- Pohl, E., Haller, J. C., Mijovilovich, A., Meyer-Klaucke, W., Garman, E. & Vasil, M. L. (2003). *Mol. Microbiol.* **47**, 903–915.
- Qi, L., Li, J., Zhang, W., Liu, J., Rong, C., Li, Y. & Wu, L. (2012). *PLoS One*, **7**, e29572.
- Rangarajan, E. S. & Izard, T. (2010). *Acta Cryst.* **F66**, 1617–1620.
- Scheffel, A., Gruska, M., Faivre, D., Linaroudis, A., Plitzko, J. M. & Schüler, D. (2006). *Nature (London)*, **440**, 110–114.
- Schultheiss, D. & Schüler, D. (2003). *Arch. Microbiol.* **179**, 89–94.
- Sheikh, M. A. & Taylor, G. L. (2009). *Mol. Microbiol.* **72**, 1208–1220.
- Studier, F. W. (2005). *Protein Expr. Purif.* **41**, 207–234.
- Trapani, S. & Navaza, J. (2008). *Acta Cryst.* **D64**, 11–16.
- Uebe, R., Voigt, B., Schweder, T., Albrecht, D., Katzmann, E., Lang, C., Bottger, L., Matzanke, B. & Schuler, D. (2011). *J. Bacteriol.* **192**, 4192–4204.
- Vagin, A. & Teplyakov, A. (2010). *Acta Cryst.* **D66**, 22–25.
- Vonnrhein, C., Blanc, E., Roversi, P. & Bricogne, G. (2007). *Methods Mol. Biol.* **364**, 215–230.
- Winn, M. D. *et al.* (2011). *Acta Cryst.* **D67**, 235–242.